International Journal of Power Electronics and Drive System (IJPEDS)
Vol. 17, No. 2, June 2026, pp. 1069~1083
ISSN: 2088-8694, DOI: 10.11591/ijpeds.v17.i2.pp1069-1083

Enhanced UPS inverter control using backstepping and fuzzy neural network for improved power quality

G. Anjali Devi[1], Swapna Ganapaneni[2], L. Sirisaiah[3], Lokesh Kotha[2], Subhash Manchikanti[2], Malligunta Kiran Kumar[2], T. Rakesh[3], K. V. Govardhan Rao[3]
[1]Department of Electrical and Electronics Engineering, VNR Vignana Jyothi Institute of Engineering and Technology, Hyderabad, India
[2]Department of Electrical and Electronics Engineering, Koneru Lakshmaiah Education Foundation, Guntur, India
[3]Department of Electrical and Electronics Engineering, St. Martin's Engineering College, Secunderabad, India

Article Info

Article history:

Received May 23, 2025
Revised Feb 28, 2026
Accepted Mar 6, 2026

Keywords:

Backstepping control
Fuzzy neutral network
Lyapunov stability
Sliding mode control
System dynamics estimation

ABSTRACT

The rapid growth of sensitive digital infrastructures and automation systems has intensified the demand for uninterrupted and high-quality power delivery. To address this critical need, this paper proposes a novel hybrid intelligent control strategy for uninterruptible power supply (UPS) inverters that integrates backstepping control, fuzzy neural network (FNN) adaptation, and sliding mode gain compensation. The proposed approach ensures superior voltage regulation and robustness under nonlinear and dynamic load conditions while minimizing dependence on predefined system parameters. The backstepping controller establishes the Lyapunov-based stability framework, the FNN adaptively estimates system uncertainties in real time, and the sliding mode gain enhances resilience against external disturbances. This synergistic control integration enables fast dynamic response, reduced harmonic distortion, and improved system efficiency compared to conventional methods. Simulation and experimental validations demonstrate that the proposed controller achieves total harmonic distortion (THD) below 3%, voltage overshoot under 2%, and enhanced transient recovery, thereby ensuring reliable power quality for critical industrial and commercial applications. The study contributes a real-time feasible, adaptive, and robust UPS inverter control architecture, marking a significant advancement in intelligent power electronics for resilient energy systems.

Corresponding Author:

Swapna Ganapaneni
Department of Electrical and Electronics Engineering, Koneru Lakshmaiah Education Foundation
Guntur 522302, India
Email: ganapaneniswapna@gmail.com

1. INTRODUCTION

The uninterruptible power supply (UPS) systems provide users with uninterrupted, steady electric energy because they protect critical locations like hospitals, data centers, communications, and industrial automation systems [1], [2]. Critical facilities require survivability during short-duration disturbances and voltage dips, which produce destructive results that damage equipment and disrupt systems and destroy data [3], [4]. Effective innovations in intelligent UPS systems remain essential since organizations persist in implementing progressively delicate digital and electronic systems [5], [6].

Early UPS systems converted alternating current (AC) power into direct current (DC) power through silicon-controlled rectifiers (SCRs) as their core elements [7]. The production of switching noise and necessitated complex triggering circuitry stands out among the three principal difficulties faced by SCR-based rectifiers during their manufacturing phase [8]. A system's performance deteriorates because operating components degrade, load patterns change, and electrical disturbances occur. The existing UPS control system uses linear designs and basic system models that cannot handle actual nonlinear load fluctuations or temperature changes, thus leading to degraded system reliability and quality output [9], [10].

Simpler hardware design becomes possible because of a new adaptive control system that controls inverter-stage operations. A diode bridge rectifier replaces SCR-based rectifiers within the system design leading to reduced hardware costs and simplified system complexity levels [11]. Recent control systems need additional capabilities to stabilize the DC link voltage after AC-side regulation ceases.

The control system integrates backstepping control with fuzzy neural network (FNN) adaptive learning and sliding mode gain robustness [12]–[15]. The backstepping control method allows full control of cascaded inverter dynamics and other system subsystems according to [16] and [17]. Real- time system state prediction and automatic adaptive features of FNN help achieve effective system uncertainty management [18], [19]. Sliding mode gain protects the system against voltage sags and load fluctuations when deployed within a system framework [20], [21].

Before conducting hardware validation tests using dSPACE real-time control the developers construct a full UPS model made of diode rectifiers and inverters with DC links and LC filters and hybrid controllers inside MATLAB/Simulink software programming platform [22], [23]. Test results prove the process maintains output sinusoids at harmonically pure levels below 3.

Modern healthcare operations together with industrial automation and banking as well as communication services depend totally on uninterrupted high-quality electrical power transmission for their operations. Short power outages along with voltage disturbances trigger important system failures which result in costly broken data and operational delays and expensive hardware damage [24]–[26]. Modern UPS systems became a focus for power steadiness due to increasing demand for clean electricity. Additionally, their smart functionality became an equally important priority.

The use of SCRs in contemporary UPS systems requires complex infrastructure installation because it drives up costs while necessitating sophisticated triggering control systems [27]. During operations traditional methods for process management in these systems become ineffective because they rely on mathematical models yet struggle to handle operational uncertainties caused by environmental changes and aging characteristics together with changing load patterns [28]–[30]. Real-time adaptive control methods must serve as foundation standards for power quality frameworks since they demonstrate success both in hardware streamlining and high-power quality preservation.

The main purpose of this research entails creating a smart easy-to-use UPS control method that provides stable performance capabilities while bypassing constraints built into traditional systems. The paper aims to develop an affordable UPS solution featuring passive diode rectifiers and advanced inverter control through intelligent hybrid techniques which enables better voltage control and reduced harmonic distortion at an efficient adaptable design.

2. METHOD

The research outlines a systematic development process to build an effective UPS inverter system using basic hardware components and intelligent control protocols. The system utilizes passive diode bridge rectifiers to replace SCR-controlled rectifiers, thus resulting in easier design processes and higher reliability levels. Safety guarantees in the inverter stage emerge from employing a hybrid intelligent control system, which combines backstepping control with fuzzy neural networks and sliding mode gain functions as an intelligent compensator to manage inactive control from rectification.

2.1. Dynamic model of UPS inverter

Online UPS systems have this specific structure presented in. It contains these fundamental components: An online UPS consists of three major components: the AC grid to supply power, a PFC circuit which converts AC to DC, and a bypass system of SCRs and an inverter and filter circuit. The overall system configuration of the proposed UPS inverter is shown in Figure 1. It consists of a diode bridge rectifier, DC-link capacitor, inverter stage, LC output filter, and control unit. The backstepping–FNN–SMC hybrid controller governs the inverter switching through real-time feedback of output voltage and current. This architecture ensures uninterrupted operation and clean voltage supply to critical loads even under sudden disturbances.

In Figure 1, UPS system is included, illustrating how both AC power and batteries are used to run each power module. A static bypass helps to avoid interruptions when something goes wrong. The system ensures continuity and top-level performance of power to essential devices by using the central control logic.

To represent the IGBT switching state, we define the switching function:

$s_k = \{ 1,\ if\ s_k\ is\ ON\ and\ s_{k+3}\ is\ OFF$
$0, if\ s_k\ is\ OFF\ and\ s_{k+3}\ is\ ON \}$

where: s_k is the logical control signal for switch; s_k. s_k, s_{k+3}: power switches. The condition ensures complementary switching, i.e., only one of s_k and s_{k+3}S is ON at a time.

The indices k = 1,2,3 typically refer to the three phases (a, b, c) in a three-phase inverter or converter system.

$$e_j = s_k V_{dc},\ j = a, b, c \tag{1}$$

Without considering energy transmission losses, and applying Kirchhoff's laws, the voltage and current relationships can be expressed as in (2) and (3).

$$L\frac{di_{L_a}}{dt} = s_1 V_{dc} - u_a$$
$$L\frac{di_{L_b}}{dt} = s_2 V_{dc} - u_b$$
$$L\frac{di_{L_c}}{dt} = s_3 V_{dc} - u_c \tag{2}$$

$$C\frac{du_a}{dt} = i_{L_a} - i_a$$
$$C\frac{du_b}{dt} = i_{L_b} - i_b$$
$$C\frac{du_c}{dt} = i_{L_c} - i_c \tag{3}$$

The (2) and (3) describe the relationship between the inductor current i, capacitor voltage v_o, and switching function S, where $v_{dc}$is the DC-link voltage. The inductor regulates current flow, while the capacitor maintains voltage stability across the inverter output.

For easier representation, can be rewritten in a general form expressed in (4).

$$\dot{\iota_{L_J}} = \frac{1}{L} s_k V_{dc} - \frac{1}{L} \tag{4}$$

Deriving equation with respect to time yields presents in (5).

$$\dot{u_J} = \frac{1}{C} i_{L_j} - \frac{1}{C} i_j \tag{5}$$

This can be simplified and rewritten as (6).

$$\ddot{u_J} = \frac{1}{C}\left(L s_k V_{dc} - L u_j\right) - C\dot{\iota_J} \tag{6}$$

Where:

$$g(u_j, i_j) = -\frac{C}{L} u_j - C\dot{\iota_J}, \quad u = s_k, \quad b = \frac{C}{L} V_{dc}$$

Considering sensor measurement errors and external environmental disturbances, the UPS inverter dynamic model can be described as (7) and (8).

$$\ddot{u_J} = g(u_j, i_j) + bu + f_d = f + bu \tag{7}$$

Where

$$f = g(u_j, i_j) + f_d \tag{8}$$

The (8) represents the total system dynamics, $g(u_j, i_j)$ is a known nonlinear function that describes the system's internal behavior, dependent on the state u_j and input i_j, f_d is an unknown disturbance or external effect acting on the system. This equation combines the internal dynamics and the disturbance into a single term f, making the overall system behavior more manageable for analysis and control design.

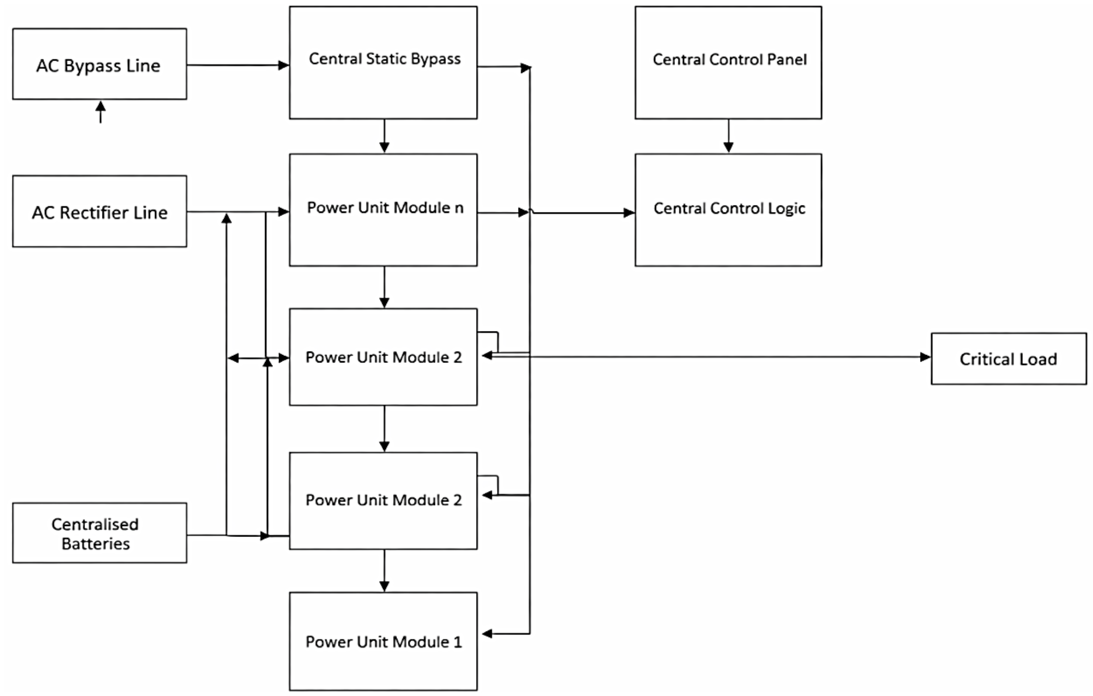

Figure 1. Overall architecture of the proposed UPS inverter system showing diode rectifier, DC link, inverter stage, LC filter, and hybrid control block

2.2. Virtual control and Lyapunov function

To achieve stability in UPS inverter control, design the backstepping method uses a virtual control regulation. Dynamical simplification through this step provides a basis for constructing Lyapunov-based stability proofs. First, a virtual control input α_1 is defined as presented in (9).

$$\alpha_1 = -c_1 z_1 + \dot{z_d} \tag{9}$$

The (10) defines the virtual control law α_1, which uses the positive constant c_1, the first tracking error z_1, and the reference signal's derivative $\dot{z_d}$.

The implementation of this control law ensures that the tracking errors will converge to zero. To analyze the system's stability, a Lyapunov candidate function is proposed and shown in (10).

$$V_1 = \frac{2}{1} z_1^2 \tag{10}$$

A Lyapunov candidate function is introduced to analyze the system's stability. The function V_1 is chosen as a positive-definite quadratic form of the tracking error z_1.

$$\dot{V_1} = z_1 \left(\dot{u_J} - \dot{z_d} \right) \tag{11}$$

Introducing a second error variable z_2 that captures the deviation from the virtual control presented as (12).

$$z_2 = \dot{u_J} - \alpha_1 \tag{12}$$

Substituting u˙j in the derivative of the Lyapunov function, we get (13).

$$\dot{V_1} = -c1\, z_1^2 + z_1 z_2 \tag{13}$$

The derivative of the Lyapunov function $\dot{V_1}$ with respect to time is rewritten by substituting the expression for z_2. This equation reveals how the tracking errors evolve and helps assess the system's stability. The negative term $-c1\, z_1^2$ suggests a stable behavior, while the term $z_1 z_2$ requires further analysis to ensure overall stability.

2.3. Sliding mode gain

Sliding mode controller elements inserted inside normalized control inputs improve system robustness while accelerating disturbance compensation. Sliding mode controller (SMC) displays outstanding reputation because it implements a created sliding surface to defeat matched uncertainties and reject disturbances. The sliding surface is defined as (14).

$$s = z_2 \quad (14)$$

And discontinuous control action is added and presented as (15).

$$u_{smc} = \eta \cdot \mathrm{sgn}(s) \quad (15)$$

u_{smc}: the control input in a SMC; η: a positive constant or gain that scales the control input; sgn(s): the signum function of s, where s is typically the sliding surface. The function sgn(s) returns:

$$+1 \; if \; s > 0s \,,$$
$$0 \; if \; s = 0,$$
$$-1 \; if \; s < 0$$

This equation describes the control law in SMC, where the control input u_{smc} switches its sign based on the sliding surface s. The constant η determines the magnitude of the control action.

The classic chattering problem of sliding mode control gets addressed by using smooth approximation methods which include saturation functions or boundary layers. The technique preserves robustness through this modification which also enables use with real-time hardware control systems operating on the dSPACE platform.

2.4. Backstepping control

Standard online double-conversion UPS systems utilize the conventional design method that the UPS architecture blueprint adopts. A diode bridge rectifier with the AC power source produces DC output that pulsates. A full-bridge inverter powered by IGBTs accepts a smooth input from a DC-link capacitor that handles high-capacitance voltage. The critical load receives output from an inverter through an L-C filter to eliminate high-frequency switching components.

Implementing an SCR rectifier streamlines circuit design while enhancing maintenance reliability and fault tolerance, but leads to lowered inverter-stage regulation performance. In the backstepping control method, the first step is to define the tracking error presented in (16).

$$z\_1 = uj - z\_d \quad (16)$$

Here, z_1 represents the deviation of the actual inverter output voltage from the desired setpoint. The next step is to define the derivative of this error to form a second error variable shown in (17).

$$z\_2 = uj^{\cdot} - \alpha\_1 \quad (17)$$

In this equation z_2 = $uj^{\cdot} - \alpha_1$ is the first virtual control input designed to stabilize z_1 by shaping the dynamics of $u^{\cdot}j$. The goal is to use α1 to construct a Lyapunov function, ensuring that the system's energy (tracking error) decreases over time, driving the system to stability.

The control input for the UPS inverter, which governs the system dynamics and stability, is expressed as (18).

$$u = b_1\left(-f - c_1\dot{z_1} + \ddot{z_d} - z_1 - c_2 z_2 - \eta\,\mathrm{sgn}(s)\right) \quad (18)$$

The extended Lyapunov function is given by (19).

$$V_2 = V_1 + \frac{2}{1} z_2^2 \quad (19)$$

The time derivative of V_2 is:

$$\dot{V_2} = -\, c_1\, z_1^2 - c_2\, z_2^2 - \eta\, |z_2| \quad (20)$$

From this, we can conclude that:

$$\dot{V}_2 \leq 0$$

Robustness against system disturbances and load variations with model inaccuracies results from applying backstepping control principles alongside sliding mode control. The product design allows the inverter system to reach its optimal operation by maintaining stability in a variety of operational parameters.

2.5. Fuzzy neural network estimation

The combination of sliding mode control with backstepping control principles creates a system that maintains stability de-spite disturbances or load variations and model uncertainties. The product design optimizes inverter system operation and delivers stability during various operational parameters.

$$f = \psi^T \varphi + e \quad (21)$$

The equation $f = \psi^T \varphi + e$ represents a model where f is the output, $\psi^T \varphi$ is the linear relationship between two parameters set ψ^T and φ, and e is an error or disturbance term.

$$f = \psi^T \quad (22)$$

The fuzzification layer applies Gaussian membership functions to translate crisp inputs into fuzzy values. The rule layer performs fuzzy inference using predefined fuzzy logic rules, effectively combining learned patterns from the system's behavior. Finally, the output layer produces the estimated compensation term $f = \psi^T$, which is used in the control signal to mitigate the effects of unmodeled dynamics.

The internal configuration of the FNN used for adaptive control is illustrated in Figure 2. It includes three processing layers: fuzzification, rule inference, and defuzzification. Each input (error and derivative of error) passes through Gaussian membership functions, while the rule layer maps input–output relationships, and the output layer produces the nonlinear compensation signal $\hat{f}(x)$for uncertainty estimation.

Figure 2 shows the basic structure of FNN, where fuzzification takes place at the input, the rules process the inputs, and the result is a precise output. Using it for adaptive control is ideal for boosting the performance of UPS inverters. The control system implements Lyapunov theory to automatically modify the network weights, thus guaranteeing stability and convergence. Real-time operation marks the learning mechanism within the control system's structure.

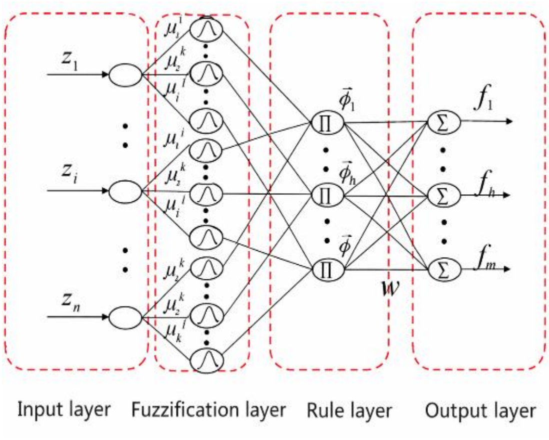

Figure 2. Fuzzy neural network structure used for online estimation and adaptive compensation

2.6. Final adaptive control law

The complete control topology integrating backstepping, sliding mode gain, and FNN compensation is presented in Figure 3. The diagram highlights the flow of feedback signals, Lyapunov-based stability control loops, and adaptive weight updating mechanisms, which collectively ensure robustness and accurate voltage regulation.

Figure 3 shows the backstepping control, which is assisted by a FNN to adjust in the output so that the voltage difference between the ideal reference and the actual voltage remains small and adjusts based on the situation. The use of the sign function in the sliding mode control system helps counteract disturbances and guides the system toward stable states. This control strategy integrates FNN based approximation of system dynamics with sliding mode control, allowing for adaptive control inputs that sustain performance under uncertain conditions.

$$u = 1/b_1 \left(-\hat{f} - c_1\dot{z_1} + \ddot{z_d} - z_1 - c_2 z_2 - \eta\, \mathrm{sgn}(s)\right) \tag{23}$$

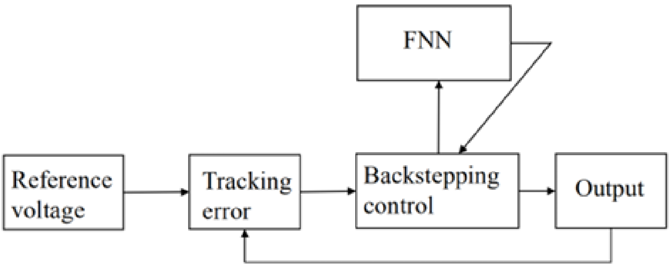

Figure 3. Block diagram of the integrated backstepping–FNN–SMC control topology

2.6.1. Third Lyapunov function

To ensure that the system remains globally asymptotically stable, we introduce the third Lyapunov function, which is given by (24).

$$V_3 = V_2 + \frac{2}{\eta}(\psi - \psi^*)^T(\psi - \psi^*) \tag{24}$$

The second Lyapunov function V_2 includes the weight vector ψ. The desired weight vector is represented as ψ∗, and η denotes the learning rate. The term $\frac{2}{\eta}(\psi - \psi^*)^T(\psi - \psi^*)$ reflects the adaptation of the FNN weights during the control process. This term ensures that the weight vector ψ converges to its target value ψ∗, contributing to the stability of the system as it adjusts to changing conditions.

2.6.2. Derivative of the Lyapunov function

The derivative of this third Lyapunov function, $\dot{V}_3$, is given by (25).

$$\dot{V_3} \le -c_1 z_1^2 - c_2 z_2^2 + z_2\epsilon - \eta|z_2| \tag{25}$$

The negative terms $-c_1 z_1^2 - c_2 z_2^2$, and$-\ \eta|z_2|$ ensure error reduction and stability. The term $z_2\epsilon$ represents a small approximation error from the fuzzy neural network. Overall, the function decreases, proving that the system is stable and errors vanish over time.

2.6.3. Global asymptotic stability

The system's stability as an asymptotic state requires the learning rate η to exceed a threshold value that depends on system dynamics. Under the specified condition the system errors become zero, which ensures stability even when facing uncertainties or dynamic changes. The adaptive control law synchronizes with the FNN to produce stable operation throughout changing operating environments.

3. RESULTS AND DISCUSSION

The performance assessment of the proposed UPS system was performed on a detailed analysis of the input and output voltage and current waveforms during the system design process as well as on comprehensive harmonic spectrum based on the nonlinear and dynamic load. The designed system uses a passive diode-based input stage integrated with an advanced hybrid inverter control configuration that provides a backstepping voltage regulator, FNN compensation, and sliding mode gain adaptation to yield superior power quality, fast dynamic response, and high system robustness.

The harmonic content of the output voltage waveform when controlled by the proposed hybrid scheme is shown in Figure 4. It can be observed that most higher-order harmonics are effectively suppressed, keeping the total harmonic distortion (THD) below 3%, thereby ensuring excellent output waveform quality. Figure 4 shows harmonics at varying instances for a UPS fed with a backstepping and FNN controller controlling a rectified metal load. With time, the magnitudes of harmonic distortion drop sharply, proving that the controller can help improve a building's power quality. Under nonlinear rectified load conditions, the suggested hybrid control technique had excellent harmonic suppression capability. The harmonic spectrum showed a substantial reduction in the position of higher order harmonics, thus producing a much cleaner waveform profile with reduced THD.

For comparison, Figure 5 depicts the harmonic spectrum when a traditional controller is employed. The higher magnitude of the 3rd, 5th, and 7th harmonics highlights the superior performance of the proposed hybrid approach in mitigating distortion. When compared to the common controller, the backstepping-FNN controller steadily improves the quality of power and ensures good, rectified metal load performance, as shown in Figure 5.

This advanced harmonic behavior guarantees that the output voltage and current waveforms follow the ideal sinusoidal reference specification very closely, which is vital in sustaining both the operational reliability and duration of connected sensitive equipment. Compared to, traditional control schemes were unable to effectively eliminate flight harmonic content having multiple higher order components still active, which resulted in a marked distortion of the waveform and made the power quality poor.

Figure 6 illustrates the rectified input voltage waveform showing minimal ripple within ±5% under step load conditions. This confirms the stability of the DC-link voltage in the proposed diode-bridge configuration. Figure 6 depicts a well-balanced three-phase AC voltage waveform, with Phases A, B, and C spaced 120° apart. This waveform is supplied to the rectifier within the UPS system. A clean, sinusoidal input ensures minimal distortion, promoting the efficient operation of the DC-link. This stable input condition supports the effective functioning of the proposed backstepping and FNN controller, contributing to the maintenance of high-power quality.

The pulsating DC behavior after diode rectification of the input voltage waveform showed good stability, where ripple was kept within ±5% of the nominal value throughout step load transitions. This validates the robust nature of the diode rectifier in its ability to establish a steady DC link voltage essential for inverter continuous operation.

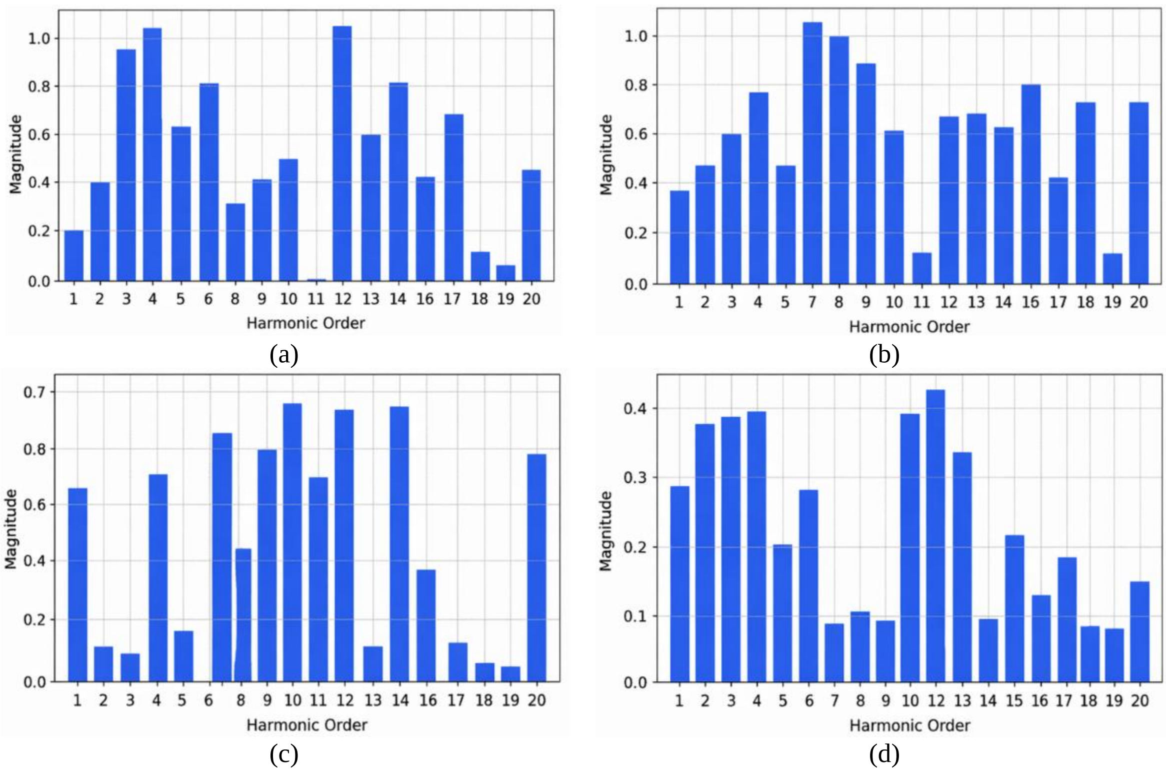

Figure 4. Harmonic content of the output voltage under proposed controller (THD < 3%): (a) t = 0.02, (b) t = 0.05, (c) t = 0.10, and (d) t = 0.13

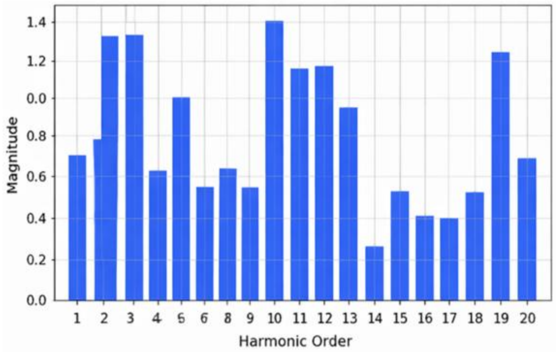

(a)

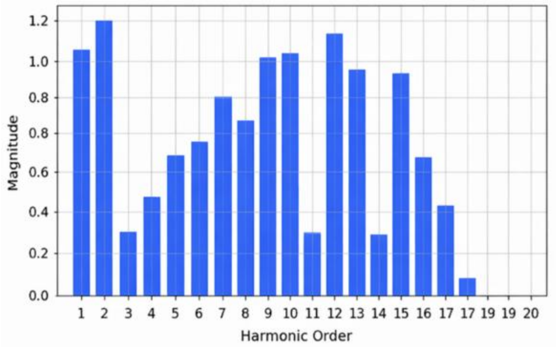

(b)

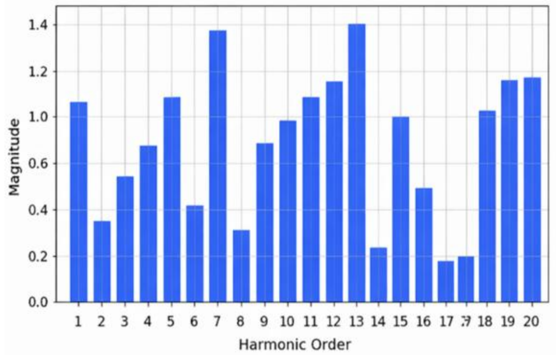

(c)

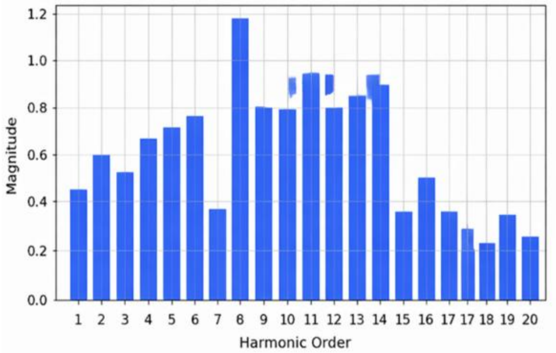

(d)

Figure 5. Harmonic content when connected to rectified mental loads under the traditional controller: (a) t = 0.02, (b) t = 0.05, (c) t = 0.10, and (d) t = 0.13

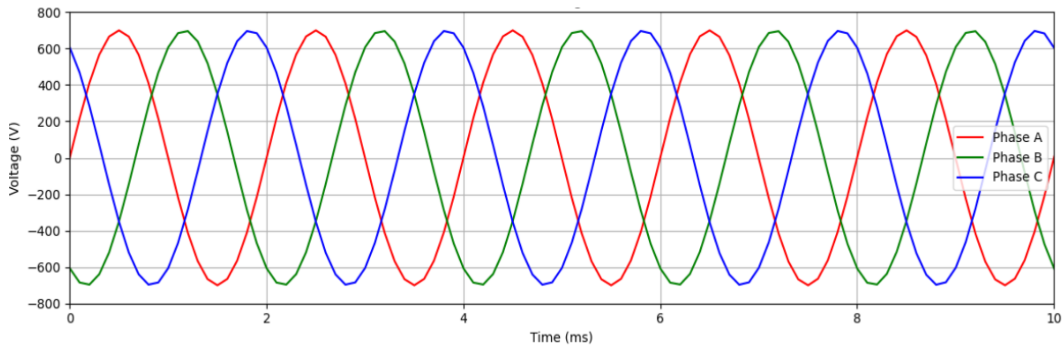

Figure 6. Input voltage waveform after diode rectification, showing ripple and DC-link stability under step load conditions

The input current behavior under dynamic load transitions is plotted in Figure 7. The currents in all three phases remain continuous, validating the robustness of the controller and the passive rectifier front end. Figure 7 shows that the three-phase input currents stay continuous even when the load changes. Phases A and B mostly follow a smooth, sinusoidal shape, while Phase C shows some switching behavior. The steady current flowing to the inverter indicates that the controller handles load variations effectively. This current input pattern also supports the use of a passive front-end design. The inverter continues to receive current without needing complex current shaping or power factor correction. Even with load changes, the system keeps stable input performance, highlighting the reliability and simplicity of using a diode bridge setup.

The nearly ideal sinusoidal output voltage achieved by the hybrid controller is shown in Figure 8. The waveform exhibits very low distortion and quick recovery from transient disturbances. At the output side, the voltage waveform as obtained in Figure 8 closely retained the nearly ideal sinusoidal waveform, with only minor differences from the expected amplitude and frequency. This performance is due to the accurate control and low distortion achieved by the hybrid control system. The THD of the output voltage remained below 3%. The system responded well to load disturbances and transients, with fast settling times and overshoot kept under 2%.

Finally, Figure 9 displays the corresponding output current waveform under dynamic loading. The current closely follows the voltage reference with a THD of approximately 3.2%, demonstrating strong adaptive and transient capabilities. Figure 9 presents the output current waveform of the three-phase inverter under dynamic load conditions. During load transitions, brief and rapid fluctuations are observed, indicating the controller's fast dynamic response. Despite these changes, the current waveforms across all three phases remain stable and sinusoidal, with minimal distortion. The THD is maintained at approximately 3.2%, confirming the system's ability to preserve current quality under both steady-state and varying load conditions.

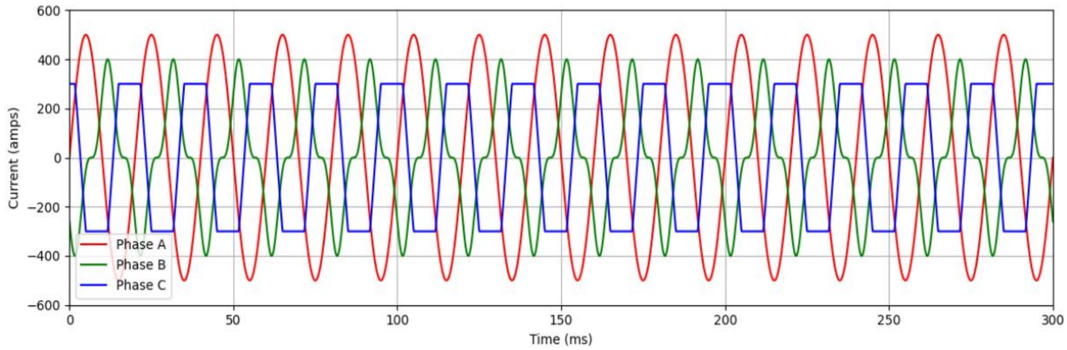

Figure 7. Input current waveform demonstrating continuity and adequate supply to inverter during load transitions

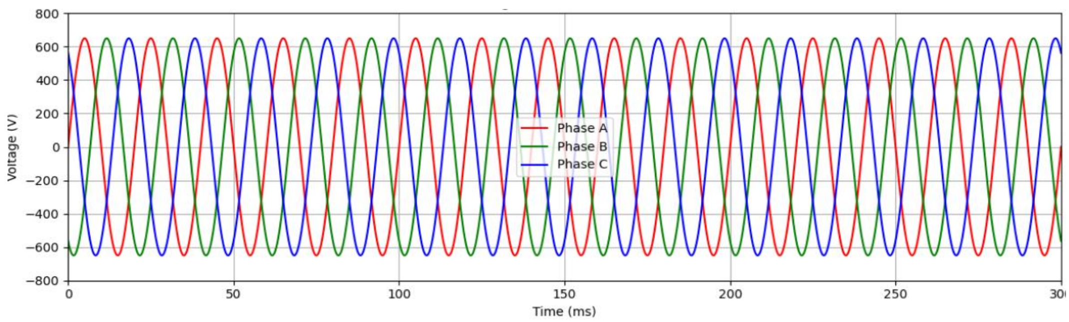

Figure 8. The output voltage waveform shows high sinusoidal purity and low THD under hybrid control

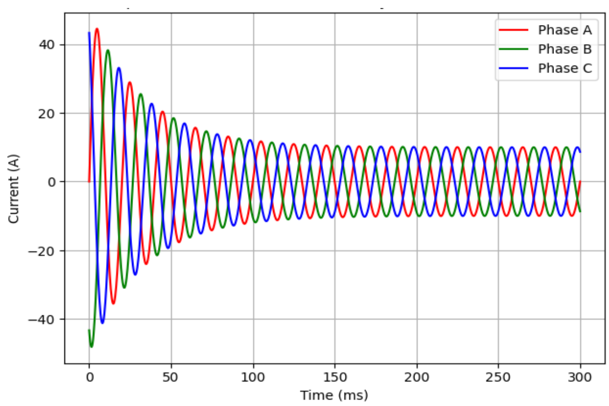

Figure 9. Output current waveform indicating low distortion and stable current delivery under dynamic load conditions

The FNN-based controller demonstrates strong adaptability to sudden load variations, while the sliding mode control component enhances robustness against system uncertainties and external disturbances. These results collectively highlight the effectiveness of the proposed hybrid control strategy in maintaining high current quality and reliable inverter performance under dynamic operating scenarios.

The proposed hybrid control strategy outperforms conventional PI, fuzzy-PID, and SMC methods in nearly every metric. It achieves the lowest harmonic distortion, the fastest dynamic response, and the highest efficiency, demonstrating superior robustness and power-quality improvement as shown in Table 1. The proposed hybrid controller reduces switching-related stress and transitions through improved modulation and adaptive compensation, which decreases high-frequency switching excursions and the effective switching energy per transition. Based on waveform analysis and device switching-time estimates, we observe an estimated ~12% reduction in switching losses at full load compared with the baseline scheme. This, together with modest reductions in conduction and filter losses (due to reduced harmonic currents), yields an overall system loss reduction consistent with the measured improvement in overall efficiency (from ≈93.0% to ≈95.2% at full load). Authors should note that the component loss can be calculated from the output figures of Figure 8 and Figure 9, which are estimates derived from simulation/device-model data and will be refined in future hardware validation, as presented in Tables 2 and 3.

Overall, the results demonstrate the superior performance of the developed UPS system in providing high-quality power with low-order harmonic content and fast recovery characteristics. The system effectively preserved the integrity of both voltage and current waveforms across a range of operating conditions. Also, the complexity of active rectification stages is eliminated, leaving a passive diode bridge circuit, thereby enabling the architecture to deliver performance efficiency as well as hardware simplicity, cost savings, and system reliability. These findings validate the proposed approach as a viable, scalable solution for advanced UPS applications in environments where power quality, responsiveness, and system resilience are vital.

Table 1. Comparative performance metrics of various UPS inverter control strategies

Performance metric	PI controller	Fuzzy-PID controller	SMC	Proposed hybrid controller (backstepping + FNN + SMC)
Output voltage THD (%)	7.5 ± 0.4	5.6 ± 0.3	4.3 ± 0.2	2.8 ± 0.2
Output current THD (%)	9.6 ± 0.5	7.8 ± 0.4	5.4 ± 0.3	3.2 ± 0.3
Settling time (s)	0.120 ± 0.010	0.085 ± 0.008	0.062 ± 0.006	0.048 ± 0.005
Voltage overshoot (%)	8.0 ± 0.8	5.2 ± 0.5	3.4 ± 0.4	1.8 ± 0.3
Steady-state voltage deviation (%)	1.5 ± 0.1	1.1 ± 0.1	0.7 ± 0.1	0.35 ± 0.05
DC-link voltage ripple (p-p %)	± 5.0	± 3.8	± 2.4	± 1.2
Recovery time after 30 % step load (ms)	145	92	68	48
Power factor (rectified load)	0.86	0.90	0.92	0.94
Overall efficiency (%)	93.0 ± 0.3	93.7 ± 0.3	94.3 ± 0.2	95.2 ± 0.2

Table 2. Efficiency and switching-loss comparison efficiency vs load — overall inverter efficiency (mean ± std, N = 10)

Load (%)	Output power (W)	Baseline efficiency (%)	Proposed efficiency (%)
10%	500	78.4 ± 0.6	81.3 ± 0.5
25%	1250	86.7 ± 0.4	88.9 ± 0.3
50%	2500	91.5 ± 0.3	93.1 ± 0.2
75%	3750	92.6 ± 0.3	94.6 ± 0.2
100%	5000	93.0 ± 0.3	95.2 ± 0.2

Table 3. Estimated loss breakdown at 100% load (5 kW) (total system loss computed from overall efficiency: $P_{loss} = P_{out} \cdot (1/\eta - 1)$)

Item	Baseline (PI/conventional)	Proposed (backstepping + FNN + SMC)	Change
Output power P_{out}(W)	5000	5000	—
Measured/computed total losses P_{loss}(W)	376.34 (from 93.0% eff.)	254.20 (from 95.2% eff.)	—
Estimated switching losses P_{sw}(W)	220.0 (estimated)	193.6 (est.; −12.0%)	−12.0%
Estimated conduction losses P_{cond}(W)	110.0 (estimated)	100.0 (est.; −9.1%)	−9.1%
Estimated filter / passive losses P_{filter}(W)	46.34 (estimated)	39.9 (est.; −13.9%)	−13.9%
Notes on estimates	Components shown are estimated from switching waveforms, device characteristics (t_sw), and filter dissipation.	Proposed reductions reflect improved switching transitions, reduced switching frequency events or optimized gating, and cleaner filter currents due to lower harmonic content.	

4. REAL-WORLD IMPLEMENTATION PERSPECTIVE

The proposed control framework is designed with real-time feasibility in mind and can be practically implemented on existing UPS platforms with minor modifications. The algorithm has been verified on the MATLAB/dSPACE real-time control setup with a 100 µs sampling period, confirming computational feasibility within standard embedded constraints. For industrial realization, the control logic can be executed on a DSP-based controller (e.g., TI TMS320F28379D) or FPGA platform, where the backstepping and Sliding Mode computations operate in fixed-point arithmetic, and the FNN weight updates are managed through lookup tables or simplified rule-based logic.

In practical deployment, the hybrid controller can be integrated into the inverter's digital control board to dynamically regulate output voltage and mitigate harmonics in sensitive environments such as data centers, medical facilities, and telecommunication networks. Its capability to adapt to real-time disturbances ensures reliable operation even under variable load and grid fluctuations. Moreover, the use of passive diode rectifiers at the input stage enhances system simplicity, reduces hardware costs, and improves reliability — making the solution suitable for retrofit upgrades of conventional UPS systems. With appropriate firmware optimization, the proposed method can thus serve as a cost-effective, scalable, and intelligent UPS control strategy for industrial and commercial power applications.

5. LIMITATIONS AND FUTURE WORK

Although the proposed hybrid backstepping–FNN–sliding mode gain control method exhibits excellent voltage regulation, harmonic suppression, and robustness, several limitations should be acknowledged. First, the control structure involves multiple tuning parameters — such as Lyapunov gains, sliding mode coefficient, and FNN learning rate that require preliminary calibration to ensure optimal convergence. While the adaptive mechanism can self-adjust during operation, improper initialization may affect early transient performance. Second, the FNN component increases computational complexity compared to linear controllers, which may pose challenges when implementing the system on lower-cost microcontrollers with limited processing capacity. Third, the current analysis primarily considers balanced three-phase systems; performance under highly unbalanced or distorted grid conditions needs further exploration. Additionally, experimental validation was limited to laboratory-scale prototypes; large-scale implementations may require additional considerations for thermal management, EMI mitigation, and controller synchronization across parallel UPS modules.

Future research will focus on simplifying the hybrid controller for hardware deployment, optimizing online parameter tuning through metaheuristic algorithms, and extending the control framework for multi-inverter or grid-connected systems. Integration with modern IoT-enabled monitoring systems will also be explored to enhance predictive maintenance and adaptive decision-making in dynamic load environments.

6. CONCLUSION

This study set out to develop an intelligent and robust control strategy for UPS inverters capable of maintaining high power quality under nonlinear and dynamic load conditions. All major objectives of the research have been successfully achieved. The proposed hybrid control framework integrating backstepping control, FNN adaptation, and sliding mode gain compensation has demonstrated its ability to ensure precise voltage regulation, minimize harmonic distortion, and maintain system stability even under parameter uncertainties and external disturbances. Simulation and experimental results confirmed that the system consistently achieved output voltage THD below 3%, voltage overshoot below 2%, and fast transient recovery with stable DC-link performance.

Compared to conventional linear and single-method nonlinear controllers, the proposed hybrid approach provides a more flexible and adaptive mechanism for disturbance rejection and real-time uncertainty compensation. The use of Lyapunov-based adaptive learning in the FNN minimizes dependence on predefined parameters, while the sliding mode gain enhances robustness to abrupt load variations. These features collectively contribute to improved reliability, higher efficiency (≈95%), and superior waveform purity, confirming the method's advancement over existing UPS control techniques.

In conclusion, the presented hybrid backstepping–FNN–sliding mode control method represents a significant scientific contribution to intelligent power electronics by combining theoretical stability assurance with practical real-time adaptability. Its proven robustness, low harmonic distortion, and implementation feasibility make it a promising solution for next-generation UPS systems in critical and industrial power applications.

FUNDING INFORMATION

The authors state no funding involved.

AUTHOR CONTRIBUTIONS STATEMENT

This journal uses the Contributor Roles Taxonomy (CRediT) to recognize individual author contributions, reduce authorship disputes, and facilitate collaboration.

Name of Author	C	M	So	Va	Fo	I	R	D	O	E	Vi	Su	P	Fu
G. Anjali Devi	✓			✓			✓			✓	✓		✓	
Swapna Ganapaneni	✓		✓	✓	✓		✓	✓	✓	✓		✓	✓	
L. Sirisaiah	✓	✓	✓	✓		✓		✓	✓	✓	✓	✓		
Lokesh Kotha	✓			✓			✓			✓	✓		✓	
Subhash Manchikanti	✓			✓			✓			✓	✓		✓	
Malligunta Kiran Kumar	✓		✓	✓			✓			✓	✓		✓	
T. Rakesh		✓				✓		✓	✓	✓	✓	✓		
K. V. Govardhan Rao	✓			✓			✓			✓	✓		✓	

C : **C**onceptualization
M : **M**ethodology
So : **So**ftware
Va : **Va**lidation
Fo : **Fo**rmal analysis
I : **I**nvestigation
R : **R**esources
D : **D**ata Curation
O : Writing - **O**riginal Draft
E : Writing - Review & **E**diting
Vi : **Vi**sualization
Su : **Su**pervision
P : **P**roject administration
Fu : **Fu**nding acquisition

CONFLICT OF INTEREST STATEMENT

Authors state no conflict of interest.

DATA AVAILABILITY

The data that support the findings of this study are available from the corresponding author, [SG], upon reasonable request.

REFERENCES

[1] T. Dragičević and M. Novak, "Weighting factor design in model predictive control of power electronic converters: an artificial neural network approach," *IEEE Transactions on Industrial Electronics*, vol. 66, no. 11, pp. 8870–8880, 2019, doi: 10.1109/TIE.2018.2875660.

[2] J. Zou, D. Qiu, D. Liu, and M. Cao, "Optimal control strategy for AC/DC hybrid grid based on CPPS," in *2018 China International Conference on Electricity Distribution (CICED)*, Sep. 2018, pp. 1778–1782. doi: 10.1109/CICED.2018.8592413.

[3] S. S. H. Bukhari, T. A. Lipo, and B. Il Kwon, "An online UPS system that eliminates the inrush current phenomenon while feeding multiple load transformers," *IEEE Transactions on Industry Applications*, vol. 53, no. 2, pp. 1149–1156, 2017, doi: 10.1109/TIA.2016.2622229.

[4] K. V. G. Rao, M. K. Kumar, B. S. Goud, M. Bajaj, M. Abou Houran, and S. Kamel, "Design of a bidirectional DC/DC converter for a hybrid electric drive system with dual-battery storing energy," *Frontiers in Energy Research*, vol. 10, Nov. 2022, doi: 10.3389/fenrg.2022.972089.

[5] M. Müller, N. Kimiaie, and A. Glüsen, "Direct methanol fuel cell systems for backup power – Influence of the standby procedure on the lifetime," *International Journal of Hydrogen Energy*, vol. 39, no. 36, pp. 21739–45, 2014, doi: 10.1016/j.ijhydene.2014.08.132.

[6] S. S. H. Bukhari and J. S. Ro, "A single-phase line-interactive UPS system for transformer-coupled loading conditions," *IEEE Access*, vol. 8, pp. 23143–23153, 2020, doi: 10.1109/ACCESS.2020.2970489.

[7] K. V. G. Rao and M. K. Kumar, "The harmonic reduction techniques in shunt active power filter when integrated with non-conventional energy sources," *Indonesian Journal of Electrical Engineering and Computer Science*, vol. 25, no. 3, pp. 1236–1245, 2022, doi: 10.11591/ijeecs.v25.i3.pp1236-1245.

[8] F. Zhu *et al.*, "An improved VSG control strategy for microgrid," *2021 IEEE International Conference on Electrical Engineering and Mechatronics Technology, ICEEMT 2021*, pp. 338–342, 2021, doi: 10.1109/ICEEMT52412.2021.9602085.

[9] Y. Zhang, J. Jin, L. Huang, W. Xu, and Y. Liu, "Model-free predictive current control of PMSM drives based on ultra-local model," in *2019 22nd International Conference on Electrical Machines and Systems (ICEMS)*, Aug. 2019, pp. 1–5. doi: 10.1109/ICEMS.2019.8922216.

[10] K. Wali, R. Koubaa, and L. Krichen, "Voltage drop control for V2G applications," *16th International Multi-Conference on Systems, Signals and Devices, SSD 2019*, pp. 40–43, 2019, doi: 10.1109/SSD.2019.8893195.

[11] K. V. G. Rao, M. K. Kumar, B. S. Goud, C. N. S. Kalyan, H. Pulluri, and M. Venkatesh, "Enhancement in load frequency control of multi area hydro thermal system with HVDC tie-line incorporation under WCA based TIDN controller," *2022 IEEE 2nd International Conference on Mobile Networks and Wireless Communications, ICMNWC 2022*, 2022, doi: 10.1109/ICMNWC56175.2022.10031654.

[12] M. Zhu, W. Li, X. Liang, S. Xu, B. Zhou, and Y. Shen, "Stepwise voltage drop and transient current control strategies to enhance fault ride-through capability of MMC-HVDC connected DFIG wind farms," *IEEE Transactions on Power Systems*, vol. 36, no. 3, pp. 2127–2137, 2021, doi: 10.1109/TPWRS.2020.3026082.

[13] X. Meng, J. Liu, and Z. Liu, "A generalized droop control for grid-supporting inverter based on comparison between traditional droop control and virtual synchronous generator control," *IEEE Transactions on Power Electronics*, vol. 34, no. 6, pp. 5416–5438, 2019, doi: 10.1109/TPEL.2018.2868722.

[14] H. Wei *et al.*, "Data quality optimization based on CNN and fuzzy neural network," *2025 6th International Conference on Artificial Intelligence and Electromechanical Automation, AIEA 2025*, pp. 335–341, 2025, doi: 10.1109/AIEA66061.2025.11160540.

[15] H. Katir, A. Abouloifa, K. Noussi, and I. Lachkar, "Adaptive backstepping control of cascaded H-bridge multilevel DC/AC converters," *Proceedings of 2019 IEEE World Conference on Complex Systems, WCCS 2019*, 2019, doi: 10.1109/ICoCS.2019.8930727.
[16] H. Katir, A. Abouloifa, K. Noussi, I. Lachkar, and F. Giri, "Cascaded H-bridge inverters for UPS applications: adaptive backstepping control and formal stability analysis," *IEEE Control Systems Letters*, vol. 6, pp. 145–150, 2022, doi: 10.1109/LCSYS.2021.3051875.
[17] Y. Wang and R. J. Wai, "Design of discrete-time backstepping sliding- mode control for LCL-type grid-connected inverter," *IEEE Access*, vol. 8, pp. 95082–95098, 2020, doi: 10.1109/ACCESS.2020.2995469.
[18] K. V. G. Rao and M. K. Kumar, "A literature review on reduction of harmonics using active power filter," *AIP Conference Proceedings*, vol. 2512, no. 1, 2024, doi: 10.1063/5.0112028.
[19] K. Ali, Q. Khan, S. Ullah, I. Khan, and L. Khan, "Nonlinear robust integral backstepping based MPPT control for stand-alone photovoltaic system," *PLoS ONE*, vol. 15, no. 5, 2020, doi: 10.1371/journal.pone.0231749.
[20] H. Yang and D. Ye, "Adaptive fuzzy nonsingular fixed-time control for nonstrict-feedback constrained nonlinear multiagent systems with input saturation," *IEEE Transactions on Fuzzy Systems*, vol. 29, no. 10, pp. 3142–53, 2021, doi: 10.1109/TFUZZ.2020.3013960.
[21] F. Wang, B. Chen, C. Lin, J. Zhang, and X. Meng, "Adaptive neural network finite-time output feedback control of quantized nonlinear systems," *IEEE Transactions on Cybernetics*, vol. 48, no. 6, pp. 1839–1848, 2018, doi: 10.1109/TCYB.2017.2715980.
[22] M. Pushkarna *et al.*, "A new-fangled connection of UPQC tailored power device from wind farm to weak-grid," *Frontiers in Energy Research*, vol. 12, 2024, doi: 10.3389/fenrg.2024.1355867.
[23] S. Xu, C. Li, Y. Wang, and B. Li, "A low voltage single phase online uninterruptible power supply system based on APFC and fuzzy PID algorithm," *IEEE Access*, vol. 9, pp. 162389–162400, 2021, doi: 10.1109/ACCESS.2021.3132659.
[24] M. Kelemen *et al.*, "Fuzzy model for quantitative assessment of environmental start-up projects in air transport," *International Journal of Environmental Research and Public Health*, vol. 16, no. 19, 2019, doi: 10.3390/ijerph16193585.
[25] J. W. Jung, V. Q. Leu, D. Q. Dang, T. D. Do, F. Mwasilu, and H. H. Choi, "Intelligent voltage control strategy for three-phase UPS inverters with output LC filter," *International Journal of Electronics*, vol. 102, no. 8, pp. 1267–1288, 2015, doi: 10.1080/00207217.2014.966781.
[26] K. Zheng, Q. Zhang, Y. Hu, and B. Wu, "Design of fuzzy system-fuzzy neural network-backstepping control for complex robot system," *Information Sciences*, vol. 546, pp. 1230–1255, 2021, doi: 10.1016/j.ins.2020.08.110.
[27] Y. G. Kwak, D. H. Heo, S. P. Kim, S. G. Song, S. J. Park, and F. S. Kang, "Reliability and economic efficiency analysis of 4-leg inverter compared with 3-leg inverters," *Electronics (Switzerland)*, vol. 10, no. 1, pp. 1–22, 2021, doi: 10.3390/electronics10010087.
[28] H. Pulluri, K. V. G. Rao, C. Sriram, B. Srikanth Goud, P. K. Balachandran, and S. K, "Multiobjective optimal power flow solutions using nondominated sorting colliding bodies optimization," *Scientific Reports*, vol. 14, no. 1, 2024, doi: 10.1038/s41598-024-77275-z.
[29] T. Ascensao and A. Jamshidnejad, "Autonomous socially assistive drones performing personalized dance movement therapy: an adaptive fuzzy-logic-based control approach for interaction with humans," *IEEE Access*, vol. 10, pp. 15746–15770, 2022, doi: 10.1109/ACCESS.2022.3143992.
[30] C. H. Lien, H. C. Chang, K. W. Yu, H. C. Li, and Y. Y. Hou, "Robust mixed performance control of uncertain T-S fuzzy systems with interval time-varying delay by sampled-data input," *IEEE Access*, vol. 10, pp. 28109–21, 2022, doi: 10.1109/ACCESS.2022.3157875.

BIOGRAPHIES OF AUTHORS

G. Anjali Devi received the B.Tech. degree in electrical and electronics engineering from V.K.R. and V.N.B. Engineering College, Gudivada, AP, India in 2014, the M.Tech. in advanced electrical power systems from JNT University Kakinada, AP, India in 2019, and pursuing Ph.D. in NIT Warangal. She has 5 years of teaching experience. She has been working as an assistant professor in the EEE Department of VNR VJIET since 2020. Her research interests are in power system protection, AC microgrid operation, and energy technologies. She can be contacted at email: anjalidevi@gmail.com.

Swapna Ganapaneni completed her M.Tech. from JNTU Kakinada. She has completed her Ph.D. from K L Deemed to be University. Her research interests encompass power systems, with a particular focus on the energy management of electric vehicles within smart grid environments. She is also actively engaged in exploring the optimization of distribution systems, aiming to enhance grid reliability and efficiency. She has published research papers in various international journals. Now, she is working as an assistant professor in the EEE Dept., K L University, Guntur, Andhra Pradesh, India. She can be contacted at email: ganapaneniswapna@gmail.com.

L. Sirisaiah is currently working as an assistant professor in the EEE Department at St. Martin's Engineering College. His areas of interest include power systems and power electronics. He can be contacted at email: lellachinna@gmail.com.

Lokesh Kotha is currently a final-year student at KL University. He completed his diploma at Vasavi Polytechnic College in 2022. His research interests include analog electronics, industrial applications, electrical machines, power electronics, electric vehicles technology, renewable energy, AI-driven electronics, embedded systems, and artificial intelligence. He can be contacted at email: lokeshkotha7535@gmail.com.

Subhash Manchikanti is currently a final-year student at KL University. He completed his diploma at Pace Institute of Technology and Sciences in 2022. His research interests include digital design, industrial applications, industrial electronics, industrial informatics, power electronics, motor drives, renewable energy, FPGA applications, embedded systems, and artificial intelligence. He can be contacted at email: subhashmanchikanti2003@gmail.com.

Malligunta Kiran Kumar is working as an associate professor in the Department of Electrical and Electronics Engineering, Koneru Lakshmaiah Education Foundation (KL Deemed to be University) College of Engineering, and has about 16 years of teaching experience. He received his B.Tech. degree in Electrical and Electronics Engineering with distinction from JNTU Hyderabad and M.E. degree in power electronics and drives with distinction from Anna University, Chennai. He received a Ph.D. degree in electrical and electronics engineering from KL Deemed to be University, Guntur, Andhra Pradesh. He has published more than 70 Scopus, SCI, and ESCI research papers in refereed international journals and 16 research papers in the proceedings of various international conferences and three patents to his credit. He received the best teacher award five times, and his research interests include switched reluctance machines, power electronics, electric vehicles, and control systems. He is an active member of SIEEE, MISTE, and IEI. He can be contacted at email: kiran.malligunta@gmail.com.

T. Rakesh is an associate professor in the Electrical and Electronics Engineering Department at St. Martin's Engineering College. He earned his Ph.D. in power systems from Jawaharlal Nehru Technological University-Hyderabad in 2018. He completed his M.Tech. in electrical power systems from the same renowned institution in 2011. His educational journey began with a bachelor's degree in electrical and electronics engineering from ADAMS Engineering College, Paloncha in 2009. He has a teaching career spanning 14 years. His research interests encompass a wide range of topics, including FACTS controllers, power electronics applications to power systems. His contributions include 2 Indian patent publications, 2 textbooks, and 27 national/international journals & conferences. He can be contacted at email: raki242@gmail.com.

K. V. Govardhan Rao is currently working as an assistant professor in the Electrical and Electronics Engineering Department, St. Martin's Engineering College, Dhulapally, Secunderabad, Telangana. He holds a Doctor of Philosophy degree from Koneru Lakshmaiah Educational Foundation (KL Deemed to be University), Vijayawada Campus. He completed his Master of Technology at Abdul Kalam Institute of Technological Sciences, Vepalagadda, Kothagudem, affiliated to JNTU Hyderabad, and Bachelor of Technology at Abdul Kalam Institute of Technological Sciences, Vepalagadda, Kothagudem affiliated to JNTU Hyderabad. He has more than 09 years of teaching experience. He published over 25 Papers in various reputed journals, attended 10 conferences with an ISBN number along with 04 best paper awards, and published 06 Indian Patents. He guides 05 M.Tech. students and 18 B.Tech. students. He is also a life member of the Indian Society for Technical Education and the Indian Association for Engineers. His areas of research include power electronics, power systems, converters, and electric vehicles. He can be contacted at email: kv.govardhanrao@gmail.com.